The Eurasia Proceedings of Science, Technology, Engineering & Mathematics (EPSTEM)
ISSN: 2602-3199

The Eurasia Proceedings of Science, Technology, Engineering and Mathematics (EPSTEM), 2025

Volume 37, Pages 689-697

ICEAT 2025: International Conference on Engineering and Advanced Technology

Synthesis and Characterization of Niobium Promoted Ni/Mesoporous MCM-41 for Potential Application in Heterogeneous-Catalyzed Reaction

May Ali Alsaffar
University of Technology - Iraq

Alyaa K. Mageed
University of Technology - Iraq

Mohamed Abdul Rahman Abdul-Ghany
University of Technology - Iraq

Bamidele Victor Ayodele
Petronas University of Technology

Abstract: The main aim of this study is to investigate the synthesis and characterization of Nb promoted Ni/MCM-41 catalyst for potential applications in heterogeneous catatyzed reaction. The catalyst was prepared using sequential wet impregnation method and characterized for its physicochemical properties using Thermogravimetric analysis (TGA), N_2 physisorption analysis, X-Ray Diffraction (XRD) analysis, Transmission Electron Microscope (TEM), Field Emission, Scanning Electron Microscope (FESEM), Energy Dispersive X-Ray Spectroscopy (EDS) and H_2-Temperature Programmed Reduction (H_2-TPR). The results revealed that the catalyst possesses a high surface area while retaining the ordered mesoporous structure of the MCM-41 support, with uniform pores centered at ~3.8 nm. The high dispersion of the crystalline Nickel oxide (NiO) was confirmed from the XRD and TEM with sizes range of 20-50 nm, across the amorphous silica framework. A strong metal-support interaction was observed from the H_2-TPR analysis which indicates the tendency of the catalyst to be thermally stable and offer high resistance against both sintering and coke deposition. The synergistic incorporation of the Nb into the Ni/MCM-41 provides a robust and highly promising catalyst for heterogeneous-catalyzed reaction.

Keywords: Niobium promoter, Mesoporous MCM-41, Nickel-based catalyst, Sequential wet impregnation

Introduction

Heterogeneous catalysis plays a pivotal role in the chemical industry, enabling more efficient and environmentally benign production processes (Mukhtar et al., 2022). Mesoporous silica materials, particularly MCM-41, have attracted significant attention as catalyst supports due to their exceptionally high surface area, uniform and tunable pore size, and thermal stability (Wei et al., 2022). These properties facilitate the high dispersion of active metal species, a crucial factor for catalytic performance (Sui et al., 2022). Nickel, being an inexpensive and active metal, is widely employed in various heterogeneous catalytic reactions, including hydrogenation, reforming, and methanation, when supported on materials like MCM-41 (Bepari & Kuila, 2020; Guo et al., 2024). The resulting Ni/MCM-41 catalysts often exhibit enhanced activity due to the well-dispersed nickel nanoparticles within the mesoporous framework (Zempulski et al., 2024).

Despite these advantages, challenges such as catalyst deactivation due to metal sintering, coke formation, and insufficient surface acidity or redox properties can limit the industrial applicability of Ni/MCM-41 (Jiang et al.,

2024; Otor et al., 2020). To address these limitations, the incorporation of a promoter is a well-established strategy to enhance the activity, selectivity, and stability of catalysts (Phung et al., 2020). Niobium (Nb) has emerged as a promising promoter in catalysis, attributed to its unique electronic and chemical properties (Ballesteros-Plata et al., 2022). The addition of niobium oxides can modify the metal-support interaction, improve the dispersion of the active phase, enhance surface acidity, and promote redox properties, which can be beneficial for a wide range of chemical transformations.

Given the individual merits of the MCM-41 support, the catalytic activity of nickel, and the promoting effects of niobium, the development of a niobium-promoted Ni/MCM-41 catalyst presents a compelling avenue for creating a robust and efficient catalytic system. This study focuses on the synthesis and characterization of such a catalyst. By introducing Nb as a promoter to the Ni/MCM-41 system, we aim to investigate the resulting structural and chemical modifications and to evaluate its potential for application in heterogeneous reactions where enhanced stability and tailored surface properties are critical for achieving high performance.

Material and Methods

Materials

The chemical precursors used for the synthesis of the catalyst include Nickel (II) Nitrate hexahydrate ($Ni(NO_3)_2{\cdot}6H_2O$) (99.9% trace metals basis, Sigma Aldrich), Niobium pentachloride ($NbCl_5$) (Sigma Aldrich), MCM-41 (Sigma Aldrich) and deionized water. All the chemicals were used without any further modification.

Catalyst Synthesis

This study employed sequential wet impregnation method for the catalyst preparation (Abdel Ghany et al., 2024). It entails the impregnation of the precursors for the active phase and the promoter into the support material in a stepwise manner (Alsaffar et al., 2021). The sequential wet impregnation method helps to have a better control over the final structure of the catalyst, thereby influencing the interaction between the metallic phases and improving the performance and stability (Aghamohammadi et al., 2017; Osakoo et al., 2015). To prepare the Nb promoted Ni/MCM-41 catalyst, a stipulated amount of $Ni(NO_3)_2{\cdot}6H_2O$ equivalent to 10wt%Ni was weighed and dissolved in about beaker containing 5 ml of deionized water. The solution is homogenized by stirring for a few minutes (Osakoo et al., 2015). The homogenized precursor solution is subsequently impregnated into the stipulated weight of MCM-41 under continuous stirring for about 5 hours to form a slurry. The slurry is subsequently placed in a petri dish for drying in an oven at 110^{o}C for 12 hours (Aghamohammadi et al., 2017). The dried slurry was subsequently placed in a ceramic crucible for calcination in a furnace at 500^{o}C for 4 hours under air flow at heating rate of 5 ^{o}C/min (Abdel Ghany et al., 2024). For the second step of the impregnation, $NbCl_5$ precursor equivalent to 2 wt% Ni was weighed and dissolve in a beaker containing 5 ml of deionized water. The solution was homogenized for a few minutes and impregnated into the calcined Ni/MCM-41 (Shakir et al., 2025). The slurry obtained was dried in the oven at 110^{o}C for 12 hours and subsequently calcined at 500^{o}C for 4 hours to obtained calcined Nb promoted Ni/MCM-41 catalyst.

Catalyst Characterization

The Nb promoted Ni/MCM-41 catalyst was characterized for its physicochemical properties using thermogravimetric analysis, X-Ray diffraction analysis, Field Emission Scanning Electron Microscope (FESEM), Energy dispersion X-ray spectroscopy (EDS) analysis, N_2 physisorption analysis, and H_2-Temperature programmed reduction (TPR) analysis. The TGA was performed using Thermogravimetry Analyzer (STA6000, Perkin Elmer). About 5mg of the catalyst sample was placed in a ceramic pan attached to a highly sensitive microbalance. A flow of N_2 is passed through the sample to study the thermal decomposition and stability in a non-reactive environment. The sample mass is continuously recorded by the thermogravimetry analyzer and the corresponding temperature. The obtained data from the analysis is plotted with time or temperature on the x-axis and percentage weigh loss on the y-axis to generate TGA curve. The crystalline phase, and the corresponding lattice parameters of the catalyst were determined using XRD. The analysis was performed on X-Ray Diffractometer (Xpert3 Powder, Panalytical). The diffractometer is made of X-ray source, sample holder, and a detector. A beam of X-rays is generated from the X-ray source which is subsequently collimated and directed to the sample.

The precise control of the sample orientation relative to the incident X-ray beam is obtained by mounting the sample on a goniometer. The intensity of the diffracted X-rays at various angles is measured by the movement of the detector in a circular path around the sample. The scans were conducted between 2θ angles of 5° to 90° with a scanning step of 0.01°/step on continuous scanning. The specific surface area and pore distribution of the catalyst was analyzed using N_2 physisorption analysis. The analysis was performed using surface area and porosity analyzer (ASAP 2020, Micromeritics). The analysis entails the adsorption of N_2 gas onto the catalyst's sample at liquid N_2 temperature of -196°C. Prior to the analysis, the sample was degassed at 300°C to eliminate any physically adsorbed contaminants from the catalyst. The specific surface area, pore size distribution, and the total pore volume can be obtained through the measurement of the amount of nitrogen gas adsorbed to and desorbed from the catalyst sample at various pressure.

The FESEM analysis of the catalyst sample was conducted to determine its morphology using Supra V55 (Zeiss). To Supra V55 FESEM analyzer is equipped with EDS detector to offer qualitative and quantitative information about the catalyst's elemental composition. High-energy electron beam is generated by the FESEM analyzer using a strong electric field. Magnetic lenses help to focus the beam and systematically scanned across the sample's surface. Signals are released from the interaction of sample with the beams revealing exceptional details of the surface topography of the catalyst sample. The signals were captured by detectors, and the intensity of the signal is mapped to form a high-resolution image that can be visualized up to nanometer scale.

The internal structure of the catalyst at the atomic scale was measured using TEM analysis. The analysis was performed on Hitachi TEM analyzer (HT7830). The TEM generates a high-energy electron beam that is focused on the sample. As the electrons pass through the catalyst, they are scattered by the internal structure. A series of electromagnetic lenses is employed to focus and magnify the transmitted electrons which is subsequently projected onto a screen or camera, producing a high-resolution image that reveals the internal morphology.

The reducibility of the catalyst was performed using H_2-TPR on Thermo-Scientific TPDRO 1100. To initiate the analysis, the catalyst sample was degassed in a flow of Argon to remove any impurities. Subsequently, a dilute hydrogen mixture with Argon is continuously flown over the catalyst sample which is being heated at a constant rate. The hydrogen consumption by the catalyst is measured using a thermal conductivity detector. The obtained data is plotted as the TPR profile that reveals the reduction peaks as specified temperatures. The peak's temperature reveals the extent of reducibility of the catalyst sample while the amount reduced is quantified using the area of the plot.

Results and Discussion

The TGA profile of the uncalcined catalysts is depicted in Figure 1. The profile shows the thermal stability of the catalyst as a function of weight loss and temperature. As shown in the TGA profile, a total of 78% weight loss occurs in three stages as summarized in Table 1 (Shakir et al., 2025). The first stage which occurs at temperature range of 25-180°C indicates the removal of physically adsorbed water from the catalyst sample since there could have been adsorbed water by the high-surface area MCM-41 support (Zempulski et al., 2024).

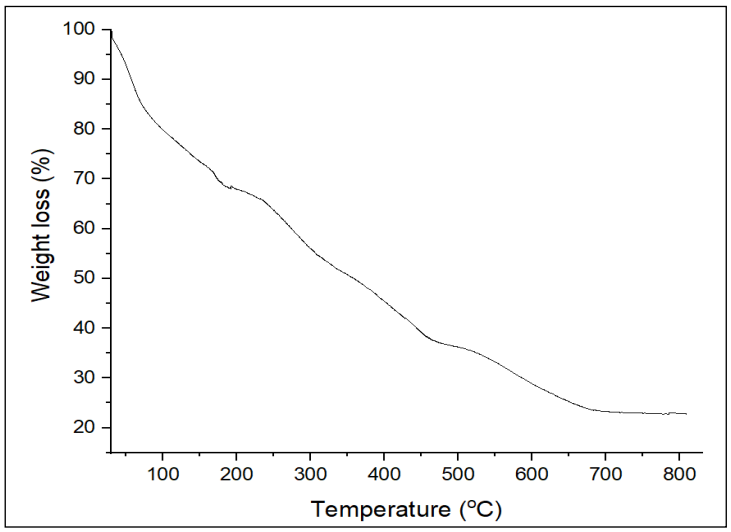

Figure 1. TGA profile of the uncalcined Nb promoted Ni/MCM-41 catalyst

The second stage, which is at temperature range of 180°C - 450°C depicts the thermal decomposition of the precursors used for the preparation of the catalyst, which results in the formation of the Ni and Nb oxides (Al-Zahrani et al., 2025). In the third stage which occurs in the temperature range of 450°C-700°C, the final residues are removed from the catalysts sample. A fully formed Nb promoted Ni/MCM-41 catalyst is obtained after 700°C.

Table 1. Summary of TGA analysis of the uncalcined Nb promoted catalyst

Temperature range (°C)	Weight loss (%)	Probable occurrence
25-180	~20	Removal of physically adsorbed water from the catalyst.
180 - 450	~45	Major decomposition of Ni precursors to its oxides; dehydroxylation of the support.
450 - 700	~13	Removal of residual precursors and final dihydroxylation.
> 700°C	0 (Plateau)	Formation of the final, thermally stable material (NiO-Nb_2O_5/MCM-41).

The N_2 physisorption analysis of the fresh catalyst to determine the specific surface area and the pore distribution is depicted in Figure 2 (a). Based on the IUPAC, the catalyst can be class as Type IV isotherm (J. Wang & Guo, 2020). The adsorption-isotherm revealed a sharp rise at $P/P^o < 0.3$ which indicates an initial monolayer-multiplayer adsorption. There is a probable occurrence of capillary condensation at $P/P^o \approx 0.3$ to 0.9 whereby the N_2 gas condenses into liquid-like state within the pores of the catalyst. The isotherm displayed a distinct hysteresis loop of Type H1 hysteresis loop whereby the desorption curve does not follow the same path as the adsorption curve (Dragan et al., 2021). The displayed of H1 hysteresis loop is typical of materials having a very narrow distribution of well-defined, uniform pores. The BET specific surface of the catalyst is estimated as 605.85 m^2/g. The pore volume of the catalyst is estimated as 0.742801 cm^3/g while the pore diameter of 5.45 nm was obtained for the catalyst.

The pore size distribution of the catalyst sample is depicted in Figure 2 (b). Most of the pores in the catalyst are uniform in size as indicated by the narrow peak. The narrow peak cluster tightly around the average diameter which implies a highly ordered and well-defined pore structure. The mesoporosity of the catalyst can further be confirmed from the peak centered at 3.8 nm which is an indication that the primary pore structure of the catalyst is within the mesoporous range of 2-50 nm. It can also be seen that there is a broader and lower-intensity distribution of pores from 5nm to 15 nm which can be attributed to textural porosity.

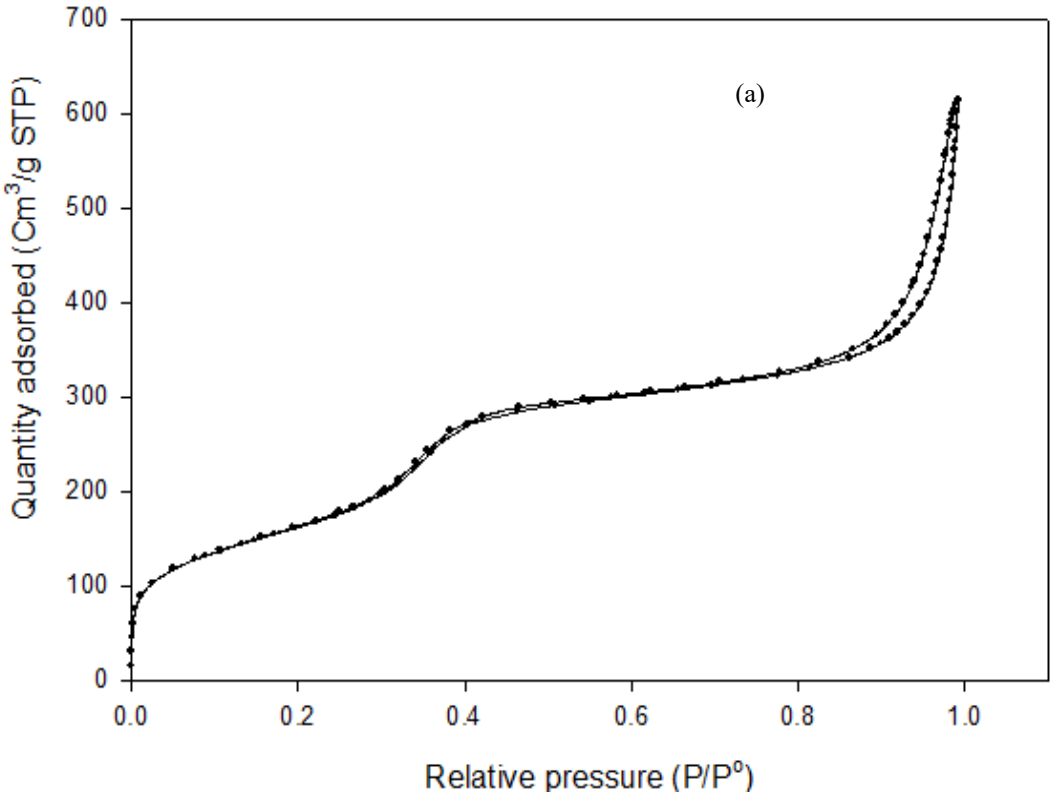

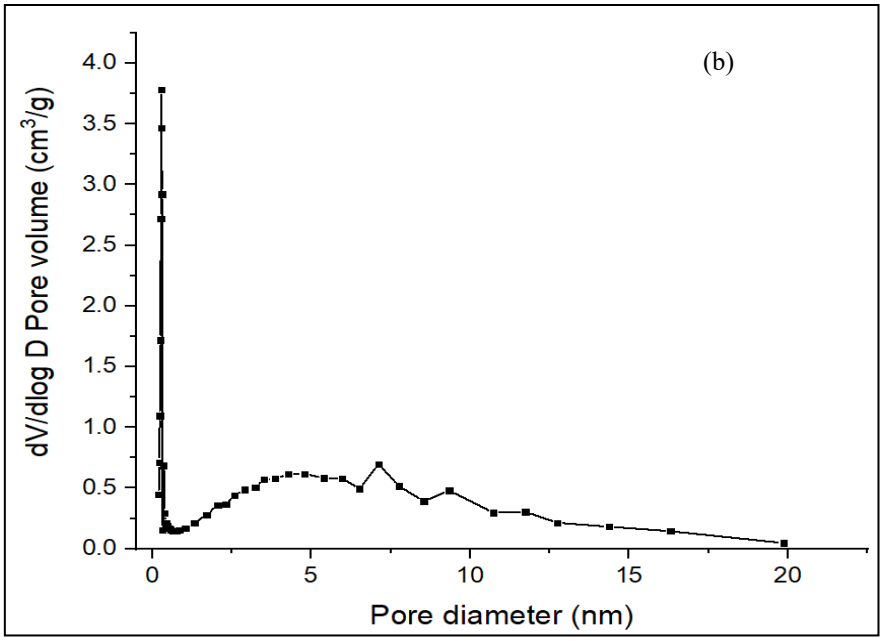

Figure 2. (a) N_2 physisorption isotherm (b) BJH pore distribution analysis of the fresh Nb promoted Ni/MCM-41 catalyst

The XRD pattern of the catalyst in Figure 3 was performed to identify the crystalline phases and to structural change in the catalyst after the impregnation of the active metals and the promoter onto the MCM-41 support. The XRD pattern of the MCM-41 sample revealed a single broad diffraction peak at 2θ = 23° which is typical of mesoporous MCM-41(Trevisan et al., 2024). The XDR pattern of the catalyst revealed the preservation of the fundamental amorphous structure of the MCM-41 after the impregnation of the Ni and Nb. The diffraction peaks at 2θ =37.2°, 43.3°, 62.9°, 75.4°, and 79.4° corresponds to the (111), (200), (220), (311), and (222) can be attributed to the crystallite NiO with faced-centered cubic structure (Tian et al., 2025). Interestingly, there is no distinct peaks that can be attributed to Nb_2O_5 phase which could implies that the nanoparticles are highly dispersed on the support due to the small amount.

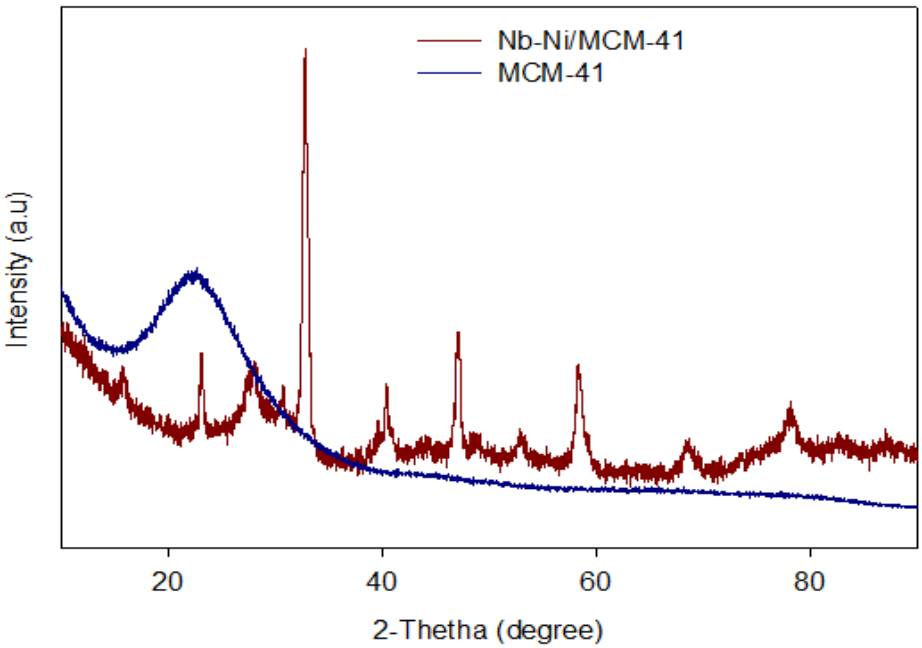

Figure 3. XRD profile of the fresh Nn promoted Ni/MCM-41 catalyst

The TEM analysis of the catalyst is depicted in Figure 4 (a). The light gray portion of the image represents the bulk of the materials that can be attributed to the MCM-41 support. This portion is less electron dense; hence it is

lighter. The presence of agglomeration in the support is typical of a fine, high-surface area materials like MCM-41. The presence of much darker nanoparticles revealed the possible dispersion of Ni and Nb on the MCM-41. The strong contrast can be attributed to the higher atomic numbers and density of Ni and Nb compared to the Si and O present in the MCM-41. The crystallinity of the nanoparticles can be visualized from the TEM image which further conforms the cubic-like shape that is consistent with the FCC crystal structure of NiO in the XRD analysis. The FESEM image of the catalyst is depicted in Figure 4 (b). The image displayed a highly porous, sponge-like surface. The FESEM image revealed that the catalyst consists of very small, roughly spherical or granular nanoparticles. The size of the nanoparticles is estimated to be in the range of 20-40 nm. The parking of the nanoparticles revealed the presence of textural porosity which is often advantageous for catalytic applications because it facilitates the diffusion of reactants to the active site on the catalyst's surface. The EDS micrograph showing the details of the elemental composition of the catalyst is depicted in Figure 4 (c). Distinct peaks corresponding to emission energies of the various elements can be observed from the spectrum. The identification of oxygen, silicon and aluminium is a confirmation of the MCM-41 support. While the presence of Ni and Nb indicates the presence of the active phase and the promoter. The compositions of the O, Si, Ni, Al, and Nb in wt% are estimated as 59.1%, 33.2%, 3.7%, 2.3%, and 1.26%, respectively. The EDS revealed that the Ni and Nb were successfully impregnated into the MCM-41 support. The high proportion of Si and O confirms that the support is the main component of the catalytic material as expected.

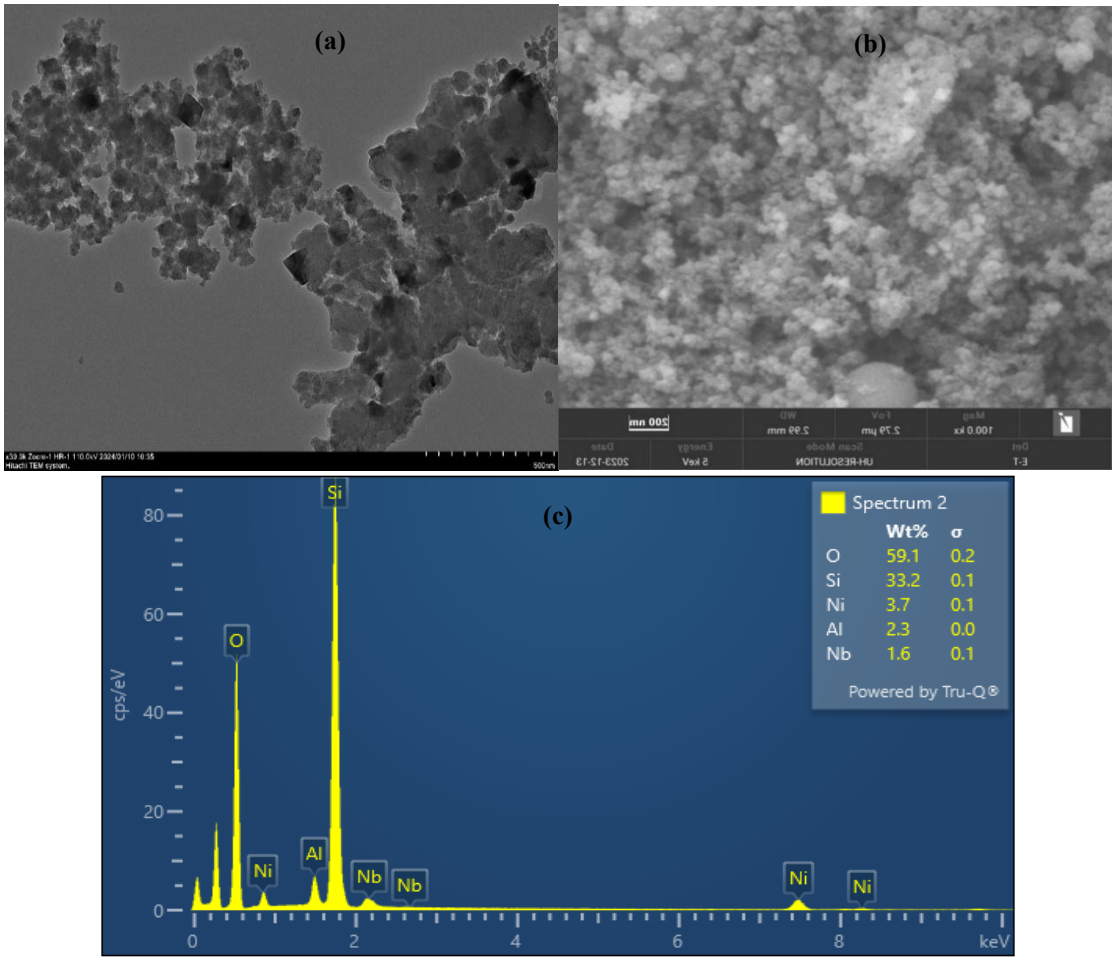

Figure 4. (a) TEM image (b) FESEM image (c) EDX micrograph of the fresh Nb promoted Ni/MCM-41 catalyst

The H_2-TPR profile to analyze the reducibility of the catalyst is depicted in Figure 5. The monitory of H_2 consumption during the analysis can help to evaluate the temperature at which the metal oxides are reduced to the metallic state. Two distinct peaks can be observed from the TPR profile which can be attributed to two types of NiO species. The peak at temperature ~320°C can be attributed to the weak interacting NiO which can be easily reduced. While the peak at temperature of ~450°C is dominant and can be attributed to the well-dispersed NiO with a strong support interaction (Meng et al., 2023; H. Wang et al., 2024). The dominance of the peak confirm that the Ni nanoparticle is highly dispersed. The strong interaction is often advantageous as it could prevent the Ni nanoparticles from sintering during high-temperature reactions. It is suggested that the catalyst be reduced insitu at temperature > 500°C to ensure complete reduction of the NiO.

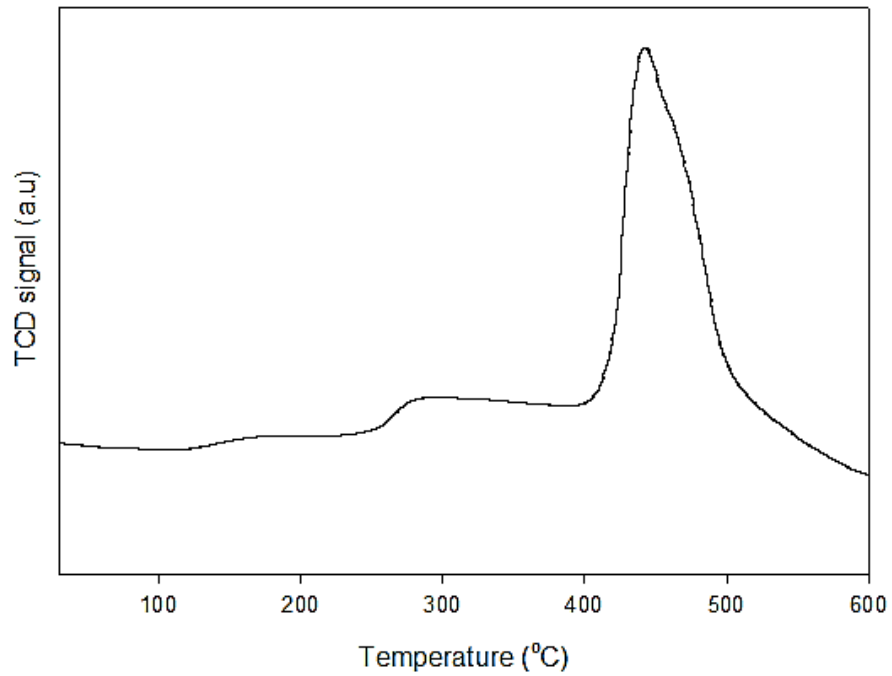

Figure 5. (a) H_2-TPR profile of the fresh Nb promoted Ni/MCM-41 catalyst

Implications for Heterogeneous-Catalyzed Reaction

The comprehensive characterization of the Nb promoted Ni/MCM-41 catalyst revealed a well-designed and promising catalyst that can be employed for heterogeneous catalyzed reaction such as the production of hydrogen via glycerol steam reforming reaction. The physicochemical properties obtained from the different characterization revealed the catalyst poised for high activity because of the maximized number of available active sites. The high surface of the MCM-41 facilitated the dispersion of the Ni and Nb as evidenced by the TEM, XRD and FESEM analyses. Moreover, high porosity is observed for the catalyst which ensures that the reactant molecules can easily reach the catalyst particles without diffusion limitations which could further enhance the overall reaction rate. The strong-metal-support interaction observed from the H_2-TPR analysis acts as an anchor, holding the Ni nanoparticles firmly thereby preventing sintering at high temperatures.

Conclusion

This study has presented a detailed characterization of Nb promoted Ni/MCM-41 catalyst for potential use in heterogeneous-catalyzed reaction. The characterization results revealed that the Nb promoted Ni/MCM-41 is a well-engineered catalyst suitable for heterogeneous-catalyzed reaction. The high surface area and uniform mesoporous structure of the MCM-41support was successfully preserved which is good for efficient mass transfer and preventing pore blockage. The characterization features highly crystalline and well-dispersed Nb and Ni nanoparticles on the MCM-41 support with an indication of a strong metal-support interaction that could prevent sintering at high temperatures. The incorporation of the Nb promoter is strategically positioned to prevent carbon deposition. The combined properties obtained from the different characterization makes the catalyst a suitable candidate for stable and active performance in heterogeneous catalyzed reactions.

Scientific Ethics Declaration

* The authors declare that the scientific ethical and legal responsibility of this article published in EPSTEM journal belongs to the authors.

Conflict of Interest

* The authors declare that they have no conflicts of interest

Funding

*There is no funding

Acknowledgements

* This article was presented as a presentation at the International Conference on Engineering and Advanced Technology (ICEAT) held in Selangor, Malaysia on July 23-24, 2025.

References

Abdel Ghany, M. A., Alsaffar, M. A., Mageed, A. K., & Sukkar, K. A. (2024). Response surface optimization of hydrogen-rich syngas production by methane dry reforming over bimetallic Mn-Ni/La2O3 catalyst in a fixed bed reactor. *International Journal of Hydrogen Energy*, *76*, 386–395.

Aghamohammadi, S., Haghighi, M., Maleki, M., & Rahemi, N. (2017). Sequential impregnation vs. sol-gel synthesized Ni/Al2O3-CeO2 nanocatalyst for dry reforming of methane: Effect of synthesis method and support promotion. *Molecular Catalysis*, *431*, 39–48.

Alsaffar, M. A., Ayodele, B. V., Ali, J. M., Abdel Ghany, M. A., Mustapa, S. I., & Cheng, C. K. (2021). Kinetic modeling and reaction pathways for thermo-catalytic conversion of carbon dioxide and methane to hydrogen-rich syngas over alpha-alumina supported cobalt catalyst. *International Journal of Hydrogen Energy*, *46*(60), 30871–30881.

Al-Zahrani, S. A., Al-Fatesh, A. S., El-Toni, A. M., Masood, N., Rajeh, S. Y., Otaibi, A. Al, & Kumar, R. (2025). Optimizing Gd-Ni/MCM-41 catalyst for H2-rich syngas production via CH4 partial oxidation. *Journal of the Taiwan Institute of Chemical Engineers*, *172*, 106133.

Ballesteros-Plata, D., Infantes-Molina, A., Rodríguez-Castellón, E., Cauqui, M. A., & Yeste, M. P. (2022). Improving noble metal catalytic activity in the dry reforming of methane by adding niobium. *Fuel*, *308*, 121996.

Bepari, S., & Kuila, D. (2020). Steam reforming of methanol, ethanol and glycerol over nickel-based catalysts-A review. *International Journal of Hydrogen Energy*, *45*(36), 18090–18113.

Dragan, G., Kutarov, V., Schieferstein, E., & Iorgov, A. (2021). Adsorption hysteresis in open slit-like micropores. *Molecules*, *26*(16), 5074.

Guo, S., Sun, Y., Zhang, Y., Zhang, C., Li, Y., & Bai, J. (2024). Bimetallic nickel-cobalt catalysts and their application in dry reforming reaction of methane. *Fuel*, *358*, 130290.

Jiang, W., Ma, X., Zhang, D., Li, Z., & Fu, P. (2024). Highly efficient catalysts for hydrogen generation through methanol steam reforming: A critical analysis of modification strategies, deactivation, mechanisms and kinetics. *Journal of Industrial and Engineering Chemistry*, *130*, 54–72.

Meng, H., Yang, Y., Shen, T., Liu, W., Wang, L., Yin, P., Ren, Z., Niu, Y., Zhang, B., Zheng, L., Yan, H., Zhang, J., Xiao, F.-S., Wei, M., & Duan, X. (2023). A strong bimetal-support interaction in ethanol steam reforming. *Nature Communications*, *14*(1), 3189.

Mukhtar, A., Saqib, S., Lin, H., Hassan Shah, M. U., Ullah, S., Younas, M., Rezakazemi, M., Ibrahim, M., Mahmood, A., Asif, S., & Bokhari, A. (2022). Current status and challenges in the heterogeneous catalysis for biodiesel production. *Renewable and Sustainable Energy Reviews*, *157*, 112012.

Osakoo, N., Henkel, R., Loiha, S., Roessner, F., & Wittayakun, J. (2015). Comparison of PdCo/SBA-15 prepared by co-impregnation and sequential impregnation for Fischer–Tropsch synthesis. *Catalysis Communications*, *66*, 73–78.

Otor, H. O., Steiner, J. B., García-Sancho, C., & Alba-Rubio, A. C. (2020). Encapsulation methods for control of catalyst deactivation: A review. *ACS Catalysis*, *10*(14), 7630–7656.

Phung, T. K., Pham, T. L. M., Nguyen, A.-N. T., Vu, K. B., Giang, H. N., Nguyen, T.-A., Huynh, T. C., & Pham, H. D. (2020). Effect of supports and promoters on the performance of Ni-based catalysts in ethanol steam reforming. *Chemical Engineering & Technology*, *43*(4), 672–688.

Shakir, H. A., Mageed, A. K., Alsaffar, M. A., & Abdel Ghany, M. A. R. (2025). Effect of process parameters and optimization of photocatalytic removal of lead from wastewater over CuZn oxide nanocomposite using response surface methodology. *Results in Chemistry*, *15*, 102255.

Sui, X., Zhang, L., Li, J., Doyle-Davis, K., Li, R., Wang, Z., & Sun, X. (2022). Advanced support materials and interactions for atomically dispersed noble-metal catalysts: From support effects to design strategies. *Advanced Energy Materials*, *12*(1), 2102556.

Tian, H., Mao, H., Wang, J., & Cheng, Y. (2025). Ga-Ni modified MCM-41@HZSM-5 core-shell zeolite for catalytic fast pyrolysis of wheat straw to produce monocyclic aromatics. *Chemical Engineering Journal*, *510*, 161707.

Trevisan, S. V. C., Oliveira, L. G., de Andrade Schaffner, R., Yamamoto, C. I., & Alves, H. J. (2024). Performance of Ni/Si-MCM-41 catalysts in CO2 methanation. *The Canadian Journal of Chemical Engineering*, *102*(8), 2724–2738.

Wang, H., Fang, Z., Wang, Y., Meng, K., & Sun, S. (2024). The study of strong metal-support interaction enhanced PdZn alloy nanocatalysts for methanol steam reforming. *Journal of Alloys and Compounds*, *986*, 174006.

Wang, J., & Guo, X. (2020). Adsorption isotherm models: Classification, physical meaning, application and solving method. *Chemosphere*, *258*, 127279.

Wei, Y., Yang, W., & Yang, Z. (2022). An excellent universal catalyst support-mesoporous silica: Preparation, modification and applications in energy-related reactions. *International Journal of Hydrogen Energy*, *47*(16), 9537–9565.

Zempulski, D. A., de Alencar, Á. O., de Andrade Schaffner, R., do Nascimento, C. T., Borba, C. E., & Alves, H. J. (2024). Effect of niobium addition over Ni/MCM-41 catalysts for dry reforming of biogas. *Environmental Science and Pollution Research*, 1-13. https://doi.org/10.1007/s11356-024-35128-2

Author(s) Information

May Ali Alsaffar
University of Technology - Iraq, Department of Chemical Engineering -Iraq, Baghdad, Iraq

Alyaa K. Mageed
University of Technology - Iraq, Department of Chemical Engineering, Baghdad, Iraq.

Mohamed Abdul Rahman Abdul-Ghany
University of Technology - Iraq, Department of Chemical Engineering, Baghdad, Iraq,

Bamidele Victor Ayodele
Petronas University of Technology, Chemical Engineering Department, , Bandar Seri Iskandar, 32610 Perak, Malaysia
Contact Email: bamidele.ayodele@utp.edu.my

To cite this article:

Alsaffar, M.A., Mageed, A.K., Abdul-Ghany, M.A.R & Ayodele, B.V. (2025). Synthesis and characterization of niobium promoted Ni/Mesoporous MCM-41 for potential application in heterogeneous-catalyzed reaction. *The Eurasia Proceedings of Science, Technology, Engineering and Mathematics (EPSTEM), 37,* 689-697.